

Crystal Structure of Lithium Molybdenum Purple Bronze $\text{Li}_{0.9}\text{Mo}_6\text{O}_{17}$

M. ONODA,* K. TORIUMI, Y. MATSUDA, AND M. SATO

*Institute for Molecular Science, Okazaki National Research Institutes,
Myodaiji, Okazaki 444, Japan*

Received January 31, 1986; in revised form April 29, 1986

The crystal structure of the molybdenum ternary oxide $\text{Li}_{0.9}\text{Mo}_6\text{O}_{17}$ is determined by single-crystal X-ray diffraction. The crystal is monoclinic with space group $P2_1/m$ and the lattice constants are $a = 12.762(2) \text{ \AA}$, $b = 5.523(1) \text{ \AA}$, $c = 9.499(1) \text{ \AA}$, $\beta = 90.61(1)^\circ$, $Z = 2$. Full-matrix least-squares refinement gives the final values of $R(F) = 0.033$ and $R_w(F) = 0.066$ for 3019 independent reflections. The unit cell contains six crystallographically independent molybdenum sites. One-third of the molybdenum atoms are located in oxygen tetrahedra, while the others are within oxygen octahedra. The structure is built up of slabs of the MoO_6 octahedra. Each slab consists of three layers of distorted ReO_3 -type MoO_6 octahedra sharing corners. The structure is rather different from that of $\text{K}_{0.9}\text{Mo}_6\text{O}_{17}$, although the layered feature is still preserved. The lithium ions are located in the large vacant sites between the slabs. By the application of Zachariasen's bond length-bond strength relation to the observed Mo-O bonds, most of the conduction electrons are found to be located in the Mo(1) and Mo(4) octahedral sites which are associated in pairs to form the $-\text{Mo}(1)-\text{O}(11)-\text{Mo}(4)-\text{O}(11)-$ double zigzag chains extending along the b -axis. Therefore the structural properties are considered to lead to the highly anisotropic electronic transport. © 1987 Academic Press, Inc.

Introduction

Transition metal ternary oxides $M_x\text{TO}_n$, where T is a transition metal atom and M is a simple metal atom, are generally called bronzes. The various properties arise from their crystal structures which are formed by the linkage of rigid units like the MoO_6 and WO_6 octahedra, for example. The electrons donated by the M atom to the TO_n cage band contribute to the electrical conduction, the natures of which strongly depend on the species of the T atoms. Many of the tungsten bronzes $M_x\text{WO}_3$ with widespread $5d$ electrons are good conductors and often exhibit superconductivity (I), while the vanadium bronzes $M_x\text{V}_2\text{O}_5$ with $3d$ electrons

have phase transitions to insulating states, or kinds of charge density wave (CDW) states due to the strong electron-phonon interactions (2).

The $4d$ electrons in the molybdenum bronzes are near the boundary between the localized and the metallic regions. They often exhibit low-dimensional conduction. For example, the molybdenum blue bronzes, $\text{K}_{0.3}\text{MoO}_3$ and $\text{Rb}_{0.3}\text{MoO}_3$ are quasi-one-dimensional conductors and undergo a Peierls transition, for which the various properties of the CDW have been subjects of recent intensive investigations (3). The transition temperatures are about 180 K for both blue bronzes, indicating that the electronic properties do not depend on the species of the M atoms but are determined only by the MoO_3 cage.

* To whom correspondence should be addressed.

The molybdenum purple bronzes $M_{0.9}Mo_6O_{17}$ ($M = Li, Na, \text{ and } K$) are another series of molybdenum bronzes (4–6). Among these, the compounds of $K_{0.9}Mo_6O_{17}$ and $Na_{0.9}Mo_6O_{17}$ undergo phase transitions to the CDW states at about 105 K (7, 8) and 70 K (9), respectively. On the other hand, $Li_{0.9}Mo_6O_{17}$ becomes superconducting at about 2 K, as Greenblatt *et al.* first found, after the anomalous upturn of the resistivity at about 25 K with decreasing temperature (10). It is known that, in contrast to the case of the molybdenum blue bronzes, the electronic properties of the molybdenum purple bronzes depend on the species of the M atoms. Thus we may be able to study superconductivity–CDW competition for these compounds. It is also

interesting to investigate the origin of the anomalous resistivity upturn with decreasing temperature followed by the superconductivity. For this, detailed information about the crystal structures of the present series of compounds is very important. However, the structure has been determined only for $K_{0.9}Mo_6O_{17}$ (11). For other compounds, it has been believed without detailed structure analyses that the structures are very similar to that of $K_{0.9}Mo_6O_{17}$. Actually their crystals appear quite similar to $K_{0.9}Mo_6O_{17}$.

In this paper, we focus mainly on the result of the structure determination of $Li_{0.9}Mo_6O_{17}$. Figure 1 shows the structure of $K_{0.9}Mo_6O_{17}$ determined by Vincent *et al.* (11). It is trigonal with the space group $P\bar{3}$.

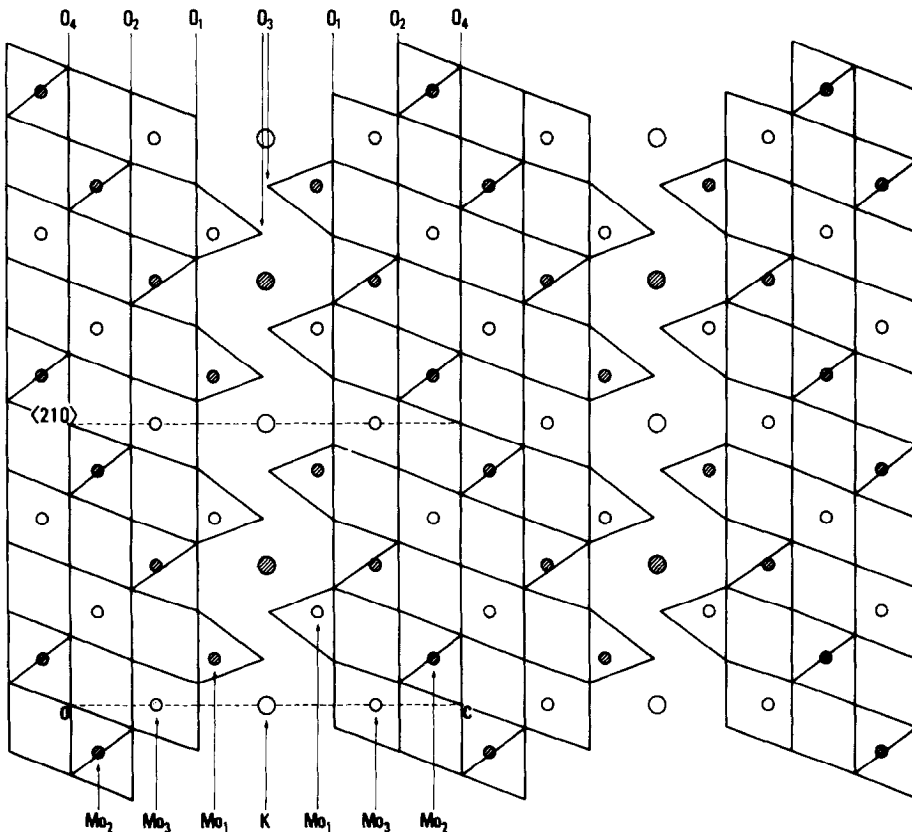


FIG. 1. Crystal structure of $K_{0.9}Mo_6O_{17}$ projected on the plane perpendicular to the a -axis after Ref. (11). Open and hatched circles indicate atomic positions at $y = 0$ and $1/2$, respectively.

It has slabs consisting of four layers of the MoO_6 octahedra separated by the KO_{12} icosahedra linked to the MoO_4 tetrahedra. Vincent *et al.* pointed out, based upon the analysis of the Mo–O bond length, that the conduction electrons are confined in the infinite layers, separated spatially, so that $\text{K}_{0.9}\text{Mo}_6\text{O}_{17}$ has quasi-two-dimensional conducting properties.

In the next section, the experimental technique and the refinement procedure will be presented. In the third section, the crystal structure of $\text{Li}_{0.9}\text{Mo}_6\text{O}_{17}$ will be described and the effective mean molybdenum valence will be estimated on the basis of the observed Mo–O bond length. The detailed results of the studies on the superconductivity and other transport properties of the series of the present compounds will be published in a separate paper (12).

Experiment and Refinement

Purple-colored single crystals of $\text{Li}_{0.9}\text{Mo}_6\text{O}_{17}$ with platelet shape were prepared by electrolysis as described by Wold *et al.* (4). Intensity data were collected at room temperature on a Rigaku AFC-5R four-circle diffractometer with graphite-monochromatized $\text{MoK}\alpha$ radiation, employing the θ – 2θ scan technique. A crystal of dimensions $0.30\text{ mm} \times 0.28\text{ mm} \times 0.11\text{ mm}$, the longest dimension being parallel to the crystallographic b -axis and the shortest parallel to the a -axis, was used for the data collection up to $2\theta = 70^\circ$. Of 6600 reflections, 3141 independent reflections with $|F_0| > 3\sigma(|F_0|)$ were obtained and used for the structure analysis. Lorentz-polarization and absorption corrections were applied. The minimal and maximal transmission factors were 0.245 and 0.559, respectively. The internal R value was $R_{\text{int}} = 0.011$. The unit cell dimensions were determined by a least-squares calculation on the basis of forty 2θ values ($25^\circ \leq 2\theta \leq 30^\circ$) measured on the

diffractometer. The crystal data are: monoclinic, space group $P2_1/m$, $Z = 2$, $a = 12.762(2)\text{ \AA}$, $b = 5.523(1)\text{ \AA}$, $c = 9.499(1)\text{ \AA}$, $\beta = 90.61(1)^\circ$, $V = 669.5(1)\text{ \AA}^3$, $\mu(\text{MoK}\alpha) = 5.43\text{ mm}^{-1}$, and $D_x = 4.24\text{ Mg m}^{-3}$.

The structure was solved from three-dimensional Patterson maps calculated by the Universal Crystallographic Computation Program System UNICS III (13) and refined by the full-matrix least-squares program RADIEL (14), where an isotropic secondary extinction effect was assumed. The weighting scheme, $w = [\sigma_c^2 + (0.015|F_0|)^2]^{-1}$, was employed, where σ_c was an estimated standard deviation for each reflection calculated from counting statistics. The oxygen and lithium atom positions were derived from difference Fourier maps. The occupancy factor of the lithium atom was fixed at 0.9, because the number is well determined by the work of various authors (4–6) and because by its refinement we could not gain any meaningful information for the atomic parameters due to the small atomic number of lithium. The refinement with isotropic temperature factors for all atoms gave $R = \sum||F_0| - |F_c||/\sum|F_0| = 0.061$. When an isotropic extinction correction was introduced in the calculation, R decreased to 0.049. The full-matrix least-squares calculation with anisotropic temperature factors gave $R = 0.043$ and $R_w = \{[\sum w(|F_0| - |F_c|)^2]/\sum w|F_0|^2\}^{1/2} = 0.069$. In order to improve the accuracy of atomic parameters, 122 strong low-angle intensities, of which extinction factors were less than 0.9, were excluded in the subsequent calculations. The final refinement was then carried out for 3019 reflections, leading to the values of R and R_w of 0.033 and 0.066, respectively. Here the atomic scattering factors and the anomalous scattering corrections were taken from "International Tables for X-Ray Crystallography," Vol. IV, in 1974 (15). A table of the observed and calculated structure factors has been deposited with the National Auxiliary Pub-

TABLE I
ATOMIC COORDINATES ($\times 10^5$) AND EQUIVALENT
ISOTROPIC THERMAL PARAMETERS (\AA^2)

		x	y	z	B_{eq}^a
Mo(1)	2e	-613(2)	25,000	23,356(3)	0.42(1)
Mo(2)	2e	14,436(3)	75,000	41,840(3)	0.40(1)
Mo(3)	2e	31,105(2)	25,000	56,755(3)	0.49(1)
Mo(4)	2e	16,635(3)	25,000	-7,938(3)	0.42(1)
Mo(5)	2e	31,980(2)	75,000	9,404(3)	0.42(1)
Mo(6)	2e	49,299(2)	25,000	19,604(3)	0.56(1)
O(1)	2e	9,143(23)	25,000	8,766(32)	0.66(5)
O(2)	2e	54,289(25)	25,000	2,127(32)	0.99(5)
O(3)	2e	59,382(24)	25,000	31,731(37)	1.45(6)
O(4)	2e	89,915(26)	25,000	40,477(33)	0.87(5)
O(5)	2e	23,138(24)	75,000	23,518(35)	0.92(5)
O(6)	2e	73,940(28)	75,000	25,932(35)	1.17(6)
O(7)	2e	55,358(22)	75,000	43,731(32)	1.01(5)
O(8)	4f	7,260(16)	50,315(32)	34,471(22)	0.83(3)
O(9)	4f	41,409(16)	51,425(34)	22,288(23)	0.97(4)
O(10)	4f	26,955(15)	50,185(32)	-383(21)	0.90(4)
O(11)	4f	91,393(15)	49,998(31)	15,323(20)	0.75(3)
O(12)	4f	26,811(16)	51,287(35)	47,264(23)	1.05(4)
Li ^b	2e	40,240(83)	75,000	40,904(148)	2.42(23)

^a $B_{\text{eq}} = \frac{1}{3} \sum_i \sum_j \beta_{ij} a_i \cdot a_j$, where β_{ij} ($i, j = 1, 2,$ and 3) are defined by the equation $\exp[-(\beta_{11}h^2 + \beta_{22}k^2 + \beta_{33}l^2 + 2\beta_{12}hk + 2\beta_{13}hl + 2\beta_{23}kl)]$.

^b Occupancy probability = 90%.

lications Service.¹ The calculations were carried out on the HITAC M-200H computer at the Computer Center of the Institute for Molecular Science.

Results and Discussion

(a) Description of the Structure

The positional and equivalent isotropic thermal parameters of the atoms are listed in Table I, and the anisotropic thermal parameters are in Table II. Figure 2 shows the crystal structure projected on the *ac* plane

¹ See NAPS document no. 04408 for 20 pages of supplementary material. Order from NAPS c/o Microfiche Publications, P.O. Box 3513, Grand Central Station, New York, N.Y. 10163. Remit in advance in U.S. funds only \$7.75 for photocopies or \$4.00 for microfiche. Outside the U.S. and Canada, add postage of \$4.50 for the first 20 pages and \$1.00 for each of 10 pages of material thereafter, \$1.50 for microfiche postage.

with the atom-numbering scheme. A stereoscopic drawing of the crystal packing viewed along the *b*-axis is given in Fig. 3. The unit cell contains six crystallographically independent molybdenum atoms, all of which are located on a mirror plane. One-third of the molybdenum atoms, labeled Mo(3) and Mo(6), are located in MoO₄ tetrahedra and the others are in MoO₆ octahedra. Chains of MoO₆ octahedra are formed parallel to the $\langle 1\ 0\ 2 \rangle$ direction. Four corner-linked octahedra and slabs with the distorted perovskite structure are formed in the *bc* plane by the chains. In contrast to K_{0.9}Mo₆O₁₇ (II) shown in Fig. 1, each slab in the present compound does not have flat surfaces. The difference between the structures of Li_{0.9}Mo₆O₁₇ and K_{0.9}Mo₆O₁₇ may be explained by the difference in the radii of the K⁺ and Li⁺ ions. The lithium ions are located in the large vacant sites between the slabs. The Li-O distances are listed in Table III and these are found to be in the usual range. The detailed lithium coordination is shown in Fig. 4.

TABLE II
ANISOTROPIC THERMAL PARAMETERS^a ($\times 10^4$)

	U_{11}	U_{22}	U_{33}	U_{12}	U_{13}	U_{23}
Mo(1)	65(2)	50(2)	47(2)		0(1)	
Mo(2)	53(2)	51(2)	47(2)		1(1)	
Mo(3)	66(2)	66(2)	55(2)		3(1)	
Mo(4)	62(1)	49(2)	50(2)		0(1)	
Mo(5)	54(2)	52(1)	53(2)		3(1)	
Mo(6)	61(2)	65(1)	86(2)		2(1)	
O(1)	89(10)	100(11)	63(10)		33(8)	
O(2)	168(13)	121(11)	89(11)		70(10)	
O(3)	138(12)	189(13)	221(15)		-58(11)	
O(4)	128(11)	143(11)	60(10)		27(8)	
O(5)	102(11)	131(11)	115(11)		55(9)	
O(6)	190(14)	162(12)	91(11)		49(10)	
O(7)	104(11)	133(11)	147(12)		-12(9)	
O(8)	115(8)	91(7)	109(7)	-41(6)	-11(6)	-17(6)
O(9)	121(8)	128(8)	120(8)	44(6)	-17(6)	4(7)
O(10)	117(8)	97(7)	128(8)	-30(7)	-9(7)	-30(7)
O(11)	108(8)	88(7)	87(7)	32(7)	-11(6)	15(7)
O(12)	132(8)	128(8)	138(8)	46(7)	-15(7)	6(7)
Li	109(35)	429(57)	381(56)		-20(35)	

^a $U_{ij} = \beta_{ij}/2\pi^2 a_i^* \cdot a_j^*$.

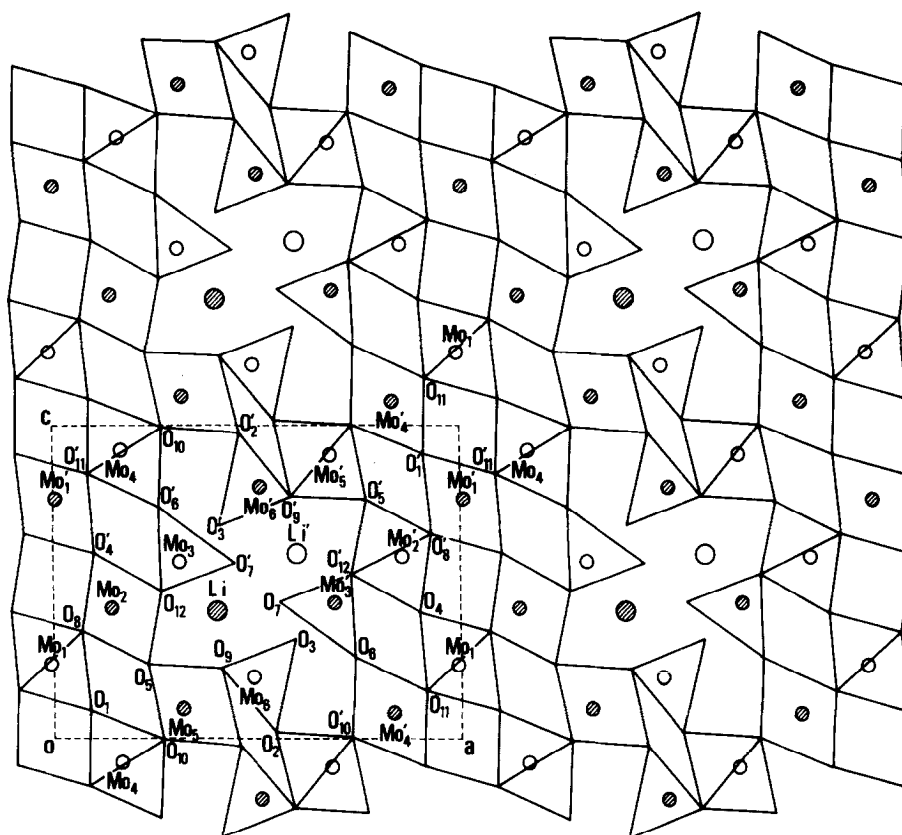


FIG. 2. Crystal structure of $\text{Li}_{0.90}\text{Mo}_6\text{O}_{17}$ projected on the ac plane. Open and hatched circles indicate atomic positions at $y = 1/4$ and $3/4$, respectively.

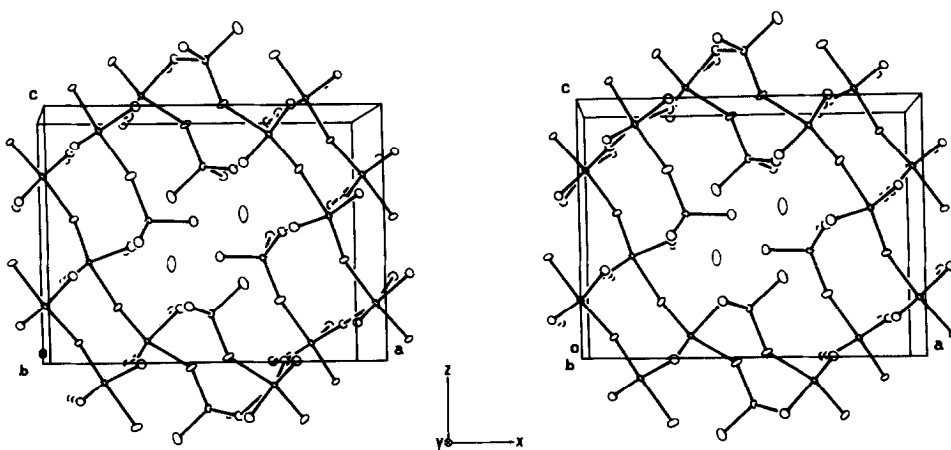


FIG. 3. Stereoscopic drawing of the crystal packing viewed along the b -axis.

(b) Estimation of the Molybdenum Valence

Selected interatomic Mo–O distances and angles are listed in Table III. The Mo–Mo distances in $\text{Li}_{0.9}\text{Mo}_6\text{O}_{17}$, $3.661(1) \sim$

$3.785(1) \text{ \AA}$, are too large to form the metallic bonds by the direct overlap of the molybdenum $4d$ wavefunctions. Thus the electronic properties of this material should be discussed on the basis of the critical overlap integral between the molybdenum and

TABLE III
SELECTED INTERATOMIC DISTANCES (\AA) AND ANGLES ($^\circ$)

Mo(1) octahedron			
Mo(1)–O(1)	1.873(3)	O(1)–Mo(1)–O(11) ^a	93.55(11)
Mo(1)–O(4) ^a	2.037(3)	O(4) ^a –Mo(1)–O(8)	83.02(11)
Mo(1)–O(8)	2.014(2)	O(4) ^a –Mo(1)–O(11) ^a	90.00(11)
Mo(1)–O(11) ^a	1.874(2)	O(8)–Mo(1)–O(8) ^b	87.93(8)
		O(8)–Mo(1)–O(11) ^a	88.19(8)
O(1)–Mo(1)–O(4) ^a	174.74(13)	O(8)–Mo(1)–O(11) ^c	172.37(8)
O(1)–Mo(1)–O(8)	93.21(11)	O(11) ^a –Mo(1)–O(11) ^c	94.89(8)
Mo(2) octahedron			
Mo(2)–O(4) ^d	1.775(3)	O(4) ^d –Mo(2)–O(12)	90.56(12)
Mo(2)–O(5)	2.074(3)	O(5)–Mo(2)–O(8)	87.01(11)
Mo(2)–O(8)	1.782(2)	O(5)–Mo(2)–O(12)	78.40(11)
Mo(2)–O(12)	2.111(2)	O(8)–Mo(2)–O(8) ^e	99.86(9)
		O(8)–Mo(2)–O(12)	90.07(8)
O(4) ^d –Mo(2)–O(5)	165.87(14)	O(8)–Mo(2)–O(12) ^e	161.93(8)
O(4) ^d –Mo(2)–O(8)	101.96(12)	O(12)–Mo(2)–O(12) ^e	76.68(8)
Mo(3) tetrahedron			
Mo(3)–O(6) ^f	1.772(3)	O(6) ^f –Mo(3)–O(7) ^f	113.44(14)
Mo(3)–O(7) ^f	1.729(3)	O(6) ^f –Mo(3)–O(12)	110.77(13)
Mo(3)–O(12)	1.792(2)	O(7) ^f –Mo(3)–O(12)	106.68(11)
		O(12)–Mo(3)–O(12) ^b	108.25(9)
Mo(4) octahedron			
Mo(4)–O(1)	1.861(3)	O(1)–Mo(4)–O(11) ^g	92.05(11)
Mo(4)–O(6) ^g	2.100(3)	O(6) ^g –Mo(4)–O(10)	85.02(11)
Mo(4)–O(10)	2.041(3)	O(6) ^g –Mo(4)–O(11) ^g	90.63(11)
Mo(4)–O(11) ^g	1.853(2)	O(10)–Mo(4)–O(10) ^b	85.94(7)
		O(10)–Mo(4)–O(11) ^g	173.37(8)
O(1)–Mo(4)–O(6) ^g	175.98(13)	O(10)–Mo(4)–O(11) ^h	88.70(8)
O(1)–Mo(4)–O(10)	92.04(11)	O(11) ^g –Mo(4)–O(11) ^h	96.36(8)
Mo(5) octahedron			
Mo(5)–O(2) ⁱ	2.076(3)	O(2) ⁱ –Mo(5)–O(10)	91.49(11)
Mo(5)–O(5)	1.762(3)	O(5)–Mo(5)–O(9)	85.75(12)
Mo(5)–O(9)	2.147(2)	O(5)–Mo(5)–O(10)	99.68(12)
Mo(5)–O(10)	1.772(2)	O(9)–Mo(5)–O(9) ^e	74.66(8)
		O(9)–Mo(5)–O(10)	91.58(8)
O(2) ⁱ –Mo(5)–O(5)	162.28(14)	O(9)–Mo(5)–O(10) ^e	164.89(8)
O(2) ⁱ –Mo(5)–O(9)	80.19(10)	O(10)–Mo(5)–O(10) ^e	101.30(9)

TABLE III—Continued

Mo(6) tetrahedron			
Mo(6)—O(2)	1.784(3)	O(2)—Mo(6)—O(3)	110.59(15)
Mo(6)—O(3)	1.718(3)	O(2)—Mo(6)—O(9)	109.81(12)
Mo(6)—O(9)	1.793(2)	O(3)—Mo(6)—O(9)	108.81(13)
		O(9)—Mo(6)—O(9) ^b	108.98(9)
Li tetradecahedron			
Li—O(3) ^d	2.599(14)	Li—O(7) ^f	3.171(7)
Li—O(5)	2.723(12)	Li—O(9)	2.202(12)
Li—O(7)	1.945(11)	Li—O(12)	2.245(9)
Cation—Cation			
Mo(1)—Mo(2)	3.785(1)	Mo(4)—Mo(5)	3.756(1)
Mo(1)—Mo(4) ^j	3.727(1)	Mo(5)—Mo(6)	3.661(1)
Mo(2)—Mo(3)	3.754(1)		

^a $-1 + x, y, z.$ ^b $x, 1/2 - y, z.$ ^c $-1 + x, 1/2 - y, z.$ ^d $1 - x, 1/2 + y, 1 - z.$ ^e $x, 3/2 - y, z.$ ^f $1 - x, -1/2 + y, 1 - z.$ ^g $1 - x, -1/2 + y, -z.$ ^h $1 - x, 1 - y, -z.$ ⁱ $1 - x, 1/2 + y, -z.$ ^j $-x, 1/2 + y, -z.$

oxygen atoms, namely the Mo—O bond length. In order to estimate the effective mean molybdenum valences, we apply the

bond length ($D(s)$) versus bond strength (s) relation proposed by Zachariasen (16) to the observed Mo—O bond lengths. This re-

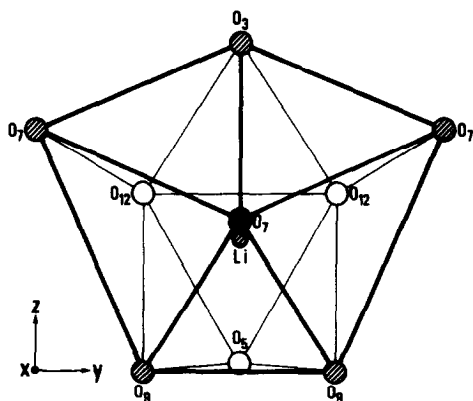


FIG. 4. The lithium atoms located in the oxygen tetradecahedron. Open, hatched, and closed circles indicate atomic positions at $x \sim 0.25, 0.42,$ and $0.55,$ respectively.

TABLE IV
BOND STRENGTHS AND EFFECTIVE MEAN
MOLYBDENUM VALENCES

	Mo(1)	Mo(2)	Mo(3)	Mo(4)	Mo(5)	Mo(6)
O(1)	1.038			1.079		
O(2)					0.544	1.379
O(3)						1.702
O(4)	0.616	1.419				
O(5)		0.547			1.479	
O(6)			1.433	0.504		
O(7)			1.643			
O(8) ^a	0.663	1.392				
O(9) ^a					0.434	1.340
O(10) ^a				0.608	1.433	
O(11) ^a	1.035					
O(12) ^a		0.486	1.344	1.107		
Mo ^{av}	5.05	5.72	5.76	5.01	5.76	5.76

^a Two symmetry-related atoms are bonded to the molybdenum atom.

lation in the molybdenum oxides is given by

$$D(s) = 1.885 - 0.314 \ln s,$$

and the effective mean valence (α) is obtained from the principle of local valence balance. The bond strengths and the effective mean molybdenum valences obtained from this relation are listed in Table IV.

It should be noted that in the case of the quasi-two-dimensional conductor $K_{0.9}Mo_6O_{17}$, the valence of the molybdenum having tetrahedral surrounding is 6+, that is, conduction electrons at this site are absent (11). In the present case, we find that all the molybdenum atoms have appreciable conduction electrons. Both the crystal structure and the conduction electron distribution suggest that $Li_{0.9}Mo_6O_{17}$ does not necessarily have two-dimensional electrical conductivity. Most of the conduction electrons are located in the Mo(1) and Mo(4) octahedral sites which are associated in pairs to form the $-Mo(1)-O(11)-Mo(4)-O(11)-$ double zigzag chains extending along the b -axis. So $Li_{0.9}Mo_6O_{17}$ seems to have quasi-one-dimensional conducting properties. This result may explain the ratios of the conductivities along the b -, c -, and a -axes of about 250 : 10 : 1 as observed by Greenblatt *et al.* (10).

Since the electronic properties of $Li_{0.9}Mo_6O_{17}$ may have quasi-one-dimensional character, this material would be expected to undergo a CDW transition. However, the resistivity anomaly observed at about 25 K has been found not to be related to the occurrence of a CDW transition by our recent investigation (12). A CDW transition accompanying the lattice distortion seems to be unfavorable indeed to the present complex structure.

In conclusion, we have solved and refined the crystal structure of $Li_{0.9}Mo_6O_{17}$. The structure has been found to be largely distorted in comparison with that of $K_{0.9}Mo_6O_{17}$ (11), although the layered structure is still preserved. The difference in the

physical properties between $Li_{0.9}Mo_6O_{17}$ and $K_{0.9}Mo_6O_{17}$ has been considered to be attributable to the crystal structures. The molybdenum valences determined from the observed Mo-O bond lengths suggest highly anisotropic conduction, which is consistent with the experimental results (10).

References

1. M. SATO, B. H. GRIER, H. FUJISHITA, S. HOSHINO, AND A. R. MOODENBAUGH, *J. Phys. C* **16**, 527 (1983).
2. H. NAGASAWA, T. ERATA, M. ONODA, H. SUZUKI, S. UJI, Y. KANAI, AND S. KAGOSHIMA, *Mol. Cryst. Liq. Cryst.* **121**, 121 (1985).
3. "Proceedings, Int. Conf. Charge Density Waves in Solids, Budapest, 1984 (G. Hutiray and J. Sólyom, Eds.), Springer-Verlag, Berlin (1985).
4. A. WOLD, W. KUNNMANN, R. J. ARNOTT, AND A. FERRETI, *Inorg. Chem.* **3**, 535 (1964).
5. J.-M. RÉAU, C. FOUASSIER, AND P. HAGENMULLER, *J. Solid State Chem.* **1**, 326 (1970).
6. W. H. MCCARROLL AND M. GREENBLATT, *J. Solid State Chem.* **54**, 282 (1984).
7. R. BUDER, J. DEVENYI, J. DUMAS, J. MARCUS, J. MERCIER, C. SCHLENKER, AND H. VINCENT, *J. Phys. (France) Lett.* **43**, L-59 (1982).
8. C. ESCRIBE-FILIPPINI, R. ALMAIRAC, R. AYROLES, C. ROUCAU, K. KONATÉ, J. MARCUS, AND C. SCHLENKER, *Philos. Mag. Part B* **50**, 321 (1984).
9. C. SCHLENKER, J. DUMAS, C. ESCRIBE-FILIPPINI, H. GUYOT, J. MARCUS, AND G. FOURCAUDOT, *Philos. Mag. Part B* **52**, 643 (1985).
10. M. GREENBLATT, W. H. MCCARROLL, R. NEIFELD, M. CROFT, AND J. V. WASZCZAK, *Solid State Commun.* **51**, 671 (1984).
11. H. VINCENT, M. GHEDIRA, J. MARCUS, J. MERCIER, AND C. SCHLENKER, *J. Solid State Chem.* **47**, 113 (1983).
12. Y. MATSUDA, M. SATO, M. ONODA, AND K. NAKAO, *J. Phys. C*, in press.
13. T. SAKURAI AND K. KOBAYASHI, *Rikagaku Kenkyusho Hokoku*, **55**, 69 (1979) (in Japanese).
14. P. COPPENS, T. N. GURU ROW, P. LEUNG, E. D. STEVENS, P. J. BECKER, AND Y. W. YANG, *Acta Crystallogr. Sect. A* **35**, 63 (1979).
15. J. A. IBERS AND W. C. HAMILTON (Eds.), "International Tables for X-Ray Crystallography," Vol. IV, Kynoch Press, Birmingham (1974).
16. W. H. ZACHARIASEN, *J. Less-Common Metals* **62**, 1 (1978).